

Universal or not: Domain walls in inhomogeneous asymmetric exclusion processes with finite resources

Sourav Pal^{1,*} and Abhik Basu^{1,†}

¹ Theory Division, Saha Institute of Nuclear Physics, a CI of Homi Bhabha National Institute, 1/AF Bidhannagar, Calcutta 700064, West Bengal, India

We study the domain walls (DW) in an asymmetric exclusion process (TASEP) with finite resources and a bottleneck. For large values of α, β , which parametrize the entry and exit rates of the TASEP lane, and with sufficiently large resources, the DWs are independent of these parameters, revealing a *hitherto unknown universality*. Unusually, these are accompanied by boundary layers in the TASEP lane. These universal DWs replace the maximal current phases in TASEPs. For smaller values of α, β , the DWs depend upon them, and hence are nonuniversal. Our studies show that both universal and nonuniversal DWs can appear for reservoirs with finite or unlimited capacity.

The role of conservation laws and their interplay with fixed obstacle to currents is paramount in a variety of physical systems, ranging from vehicular or pedestrian traffic along closed network of roads with blockages [1, 2], ribosome translocations along messenger RNA (mRNA) loops in biological cells [3–5] and closed arrays of quantum dots [6]. Totally asymmetric simple exclusion process (TASEP) is one of the most extensively studied one-dimensional (1D) nonequilibrium models [7–9] in this context. Originally proposed to study protein synthesis in eukaryotic cells [10], TASEP has subsequently emerged as a paradigmatic 1D model for nonequilibrium phase transitions in open boundary systems [7–9, 11–13]. TASEP in an inhomogeneous ring or a closed network can display macroscopically uniform or nonuniform steady states due to the interplay between particle number conservation (PNC) and inhomogeneities [14–24]. More recently, considerations of the finite availability of ribosomes in the protein synthesis processes in cells [25] have led to models consisting of one or more TASEP lanes connected to a particle reservoir at its both ends, to study the role of finite resources in mRNA synthesis in cells, revealing the role of global PNC [26–32].

In this Letter, we propose and study a conceptual model based on TASEP [7] connected to a particle reservoir to understand the mutual interplay between conserved finite resources, directed motion and localized steric hindrance (a point defect), which gives rise to nontrivial steady states. We use it to explore universality in the domain wall (DW) structures and phase diagrams for the nonequilibrium steady states in this model. Our model construction is principally motivated by protein synthesis by ribosomes in eukaryotic cells. It is known that FMRP (a polyribosome-associated neuronal RNA-binding protein) can stall ribosome translocation, or, the slowdown of a translating ribosome upon encountering a rare “slow codon” or “pause sites” (which have distinct biological functions [33–35]) in the mRNA due to the low concentration of the corresponding tRNA [36]. Our work should be useful for understanding the generic “universal” features in the phenomenologies of ribosome translo-

cations along closed mRNA loops [36] with slow codons inhibiting ribosome translocations [33–41] and also traffic jams or congestion in urban transport networks with multiple road blocks [42, 43].

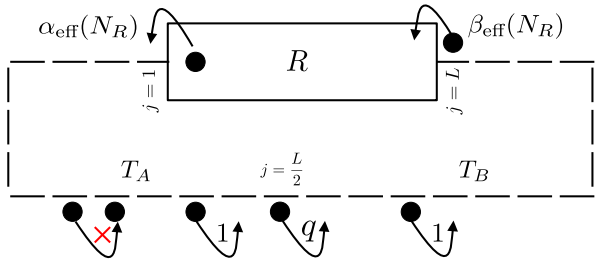


FIG. 1: A 1D lattice executing TASEP with a point defect having hopping rate $q < 1$ is connected to a particle reservoir R at its both ends. Effective entry and exit rates, α_{eff} and β_{eff} respectively, depend explicitly on reservoir population, N_R . Hopping rate throughout the lattice is set to unity except at the defect. See text.

Our model consists of a TASEP on a 1D lattice with L sites ($j = 1, 2, \dots, L$), each with unit hopping rate, except at the defect site at $j = L/2$, where hopping rate $q < 1$ [44]; see Fig. 1 for a schematic model diagram. Here, α_{eff} and β_{eff} , the effective entry and exit rates respectively, are parametrized by

$$\alpha_{\text{eff}}(N_R) = \alpha f(N_R), \quad (1)$$

$$\beta_{\text{eff}}(N_R) = \beta(1 - f(N_R)), \quad (2)$$

$$f(N_R) = N_R/N^* \in [0, 1]. \quad (3)$$

Function $f(N_R)$, a monotonic function of reservoir population N_R , describes the TASEP-reservoir couplings [26, 29, 30], N^* is a normalization factor; $\alpha, \beta \geq 0$. These choices ensure that α_{eff} goes up (reduces) with increase (decrease) in N_R , while β_{eff} behaves oppositely [29–32]. We define $\mu \equiv N_0/L$, where $N_0 \equiv N_R + \sum_{j=1}^L n_j$ is the total particle number, a constant of motion, with $n_j = 0, 1$, the occupation number of site j . The phases in the model and the associated transitions are parametrized by α, β, μ, q . The parameters α, β control the mutual

interplay between the “supply” and “demand” in finite resources systems, e.g., mRNA translation [45].

As specific examples, we choose (i) Case I: $N^* = L$ and (ii) Case II: $N^* = N_0$. From the positivity of β_{eff} and PNC, we must have (i) $N_0 \leq 2L$ or $0 \leq \mu \leq 2$ in Case I, corresponding to a finite carrying capacity of the reservoir for a given size L of the TASEP lane, (ii) no such constraint on N_0 appears in Case II, letting the model accommodate any number of particle, i.e., μ can be any positive number, corresponding to unrestricted carrying capacity of the reservoir; see also Refs. [30, 31] in this context. Only Case I (but not Case II) admits the particle-hole symmetry: $\alpha \leftrightarrow \beta$ and $\mu \leftrightarrow 2 - \mu$.

We show that generically for sufficiently large α, β and μ , the DWs that are enforced by the bottleneck in the TASEP lane are *universal*, i.e., independent of α, β and μ , *always* located at the mid point of the TASEP lanes, with their heights being dependent *solely* on q . Rather intriguingly, such a DW is necessarily associated with a pair of boundary layers (BLs) at the two ends of the TASEP lane, in contrast to TASEPs with open boundaries [12] or finite resources [26–32]. Thus measurement of such a DW tells us *nothing* about the model parameters (except q) and the choice of f , reminiscent of universal critical phenomena [46]. Identification of this DW phase, dubbed the universal DW (UDW) phase, which replaces the maximal current (MC) phase, and role of *two* BLs in UDW formation are the principal results in this Letter. For other choices of α, β , more conventional DWs without BLs emerge. In the phase space these two types of DW regions are separated by a surface with a pair of *nonuniversal delocalized domain walls* (DDWs). These results are general, holding for reservoirs with restricted (Case I) and unrestricted (Case II) carrying capacities.

For a very low μ , the bulk of the TASEP lane is in its low density (LD) phase. As μ rises, it moves to DW phases, controlled either by the defect or the reservoir, eventually reaching the high density (HD) phase for high μ . These qualitative pictures are shown in the Movies 1 and 2 in the Supplemental Material (SM) [47]. See phase diagrams in Fig. 2 in the α - β plane for various values of μ and with $q = 0.1$ for both $N^* = L, N_0$, which are very different from that for an open TASEP [12].

Partly related models and studies can be found in Ref. [48], focusing on the steady states with resources-dependent hopping rates and a slow site, and Ref. [49], discussing DWs. With $N^* = N_0$ and $q = 1$, our model reduces to that studied in Ref. [29].

To calculate the phases and the phase diagrams, we employ mean-field theory (MFT) [12] to the TASEP lane by assuming it to consist of two segments T_A and T_B with their effective entry and exit rates, connected by defect at $j = L/2$. MFT results are corroborated by extensive Monte Carlo simulations (MCS). In the following, we denote the mean density at site j by the time-average of occupation number, i.e., $\rho_j = \langle n_j \rangle$. Introducing a

quasi-continuous coordinate $x \equiv j/L$ in the thermodynamic limit $L \rightarrow \infty$, with $0 \leq x \leq 1$, we now define $\rho_m(x) \equiv \langle \rho_j^m \rangle$ as the local density, where $\langle \dots \rangle$ implies temporal averages in the steady states; $m = A, B$.

With $(\alpha_{\text{eff}}, \beta_A)$ as the effective entrance and exit rates, respectively, for T_A and $(\alpha_B, \beta_{\text{eff}})$ for T_B , stationary current conservation at $j = L/2$ and $j = (L/2) + 1$ gives

$$\beta_A = q(1 - \rho_{(L/2)+1}), \quad \alpha_B = q\rho_{L/2}. \quad (4)$$

Additionally, current through the defect site reads

$$J_d = q\rho_{L/2}(1 - \rho_{(L/2)+1}) = \alpha_B\beta_A/q. \quad (5)$$

Denoting the steady state mean densities and currents of segments T_A and T_B as ρ_A, J_A and ρ_B, J_B respectively, current conservation $J_A = J_B = J_d$ gives $\rho_A = \rho_B$, or $\rho_A + \rho_B = 1$. In analogy to an open TASEP, bulk density in the LD-LD phase in T_A is $\rho_A = \alpha_{\text{eff}}(N_R) = \alpha f(N_R)$ and in T_B is $\rho_B = \alpha_B = \rho_A$ (by current conservation), and are reservoir-controlled. By using Eq. (4) with PNC

$$\rho_{\text{LD-LD}} = \begin{cases} \mu\alpha/(1 + \alpha), & N^* = L, \\ \mu\alpha/(\mu + \alpha), & N^* = N_0. \end{cases} \quad (6)$$

vanishing, unsurprisingly, for $\mu \rightarrow 0$. The defect imposes only a local jump of $h = \alpha_{\text{eff}}(1-q)/q > 0$ with a vanishing thickness in the thermodynamic limit behind it, obtained by using current conservation in the state state [16].

The point defect can impose a DW behind it for larger μ , connecting LD and HD segments with densities ρ_{LD} and ρ_{HD} respectively. Stationary current conservation across the point defect gives [14, 19]

$$\rho_{\text{LD}} = q/(1 + q), \quad \rho_{\text{HD}} = 1 - \rho_{\text{LD}} = 1/(1 + q). \quad (7)$$

Since $q \neq 1$, $\rho_{\text{HD}} > \rho_{\text{LD}}$, meaning *if* the defect controls the steady state, there cannot be a maximal current phase, as mentioned above.

Qualitatively, upon raising N_0 or μ , ρ_{LD} rises (Eq. (6)), eventually reaching $\rho_{\text{LD}} \equiv \alpha_{\text{eff}} = q/(1 + q)$. This is the beginning of a *localized domain wall* (LDW) in T_A at $x = 1/2$, giving the DW-LD phase. With $\Theta(x) = 1(0)$ when $x > (<)0$, for an LDW $\rho(x) = \rho_{\text{LD}} + \Theta(x - x_{w_1})(\rho_{\text{HD}} - \rho_{\text{LD}})$, where ρ_{LD} and ρ_{HD} , are as given in (7), and x_{w_1} is the LDW position. PNC gives

$$x_{w_1} = \begin{cases} [(1/2 - \mu)(1 + q) + q/\alpha]/(1 - q), & N^* = L, \\ [(1/2 - \mu)(1 + q) + \mu q/\alpha]/(1 - q), & N^* = N_0. \end{cases} \quad (8)$$

Substituting $x_{w_1} = 1/2$ in Eq. (8) gives the boundary between LD-LD and DW-LD phases: $\mu\alpha/(1 + \alpha) = q/(1 + q)$ for $N^* = L$, and $\mu\alpha/(\mu + \alpha) = q/(1 + q)$ for $N^* = N_0$ (see Figs. 2(a)-2(e)). As μ or α increases further (with other parameters fixed), more particles enter the TASEP lane, pushing the LDW towards $x = 0$ keeping α_{eff} fixed, until $x_{w_1} = 0$ marks the onset of the UDW

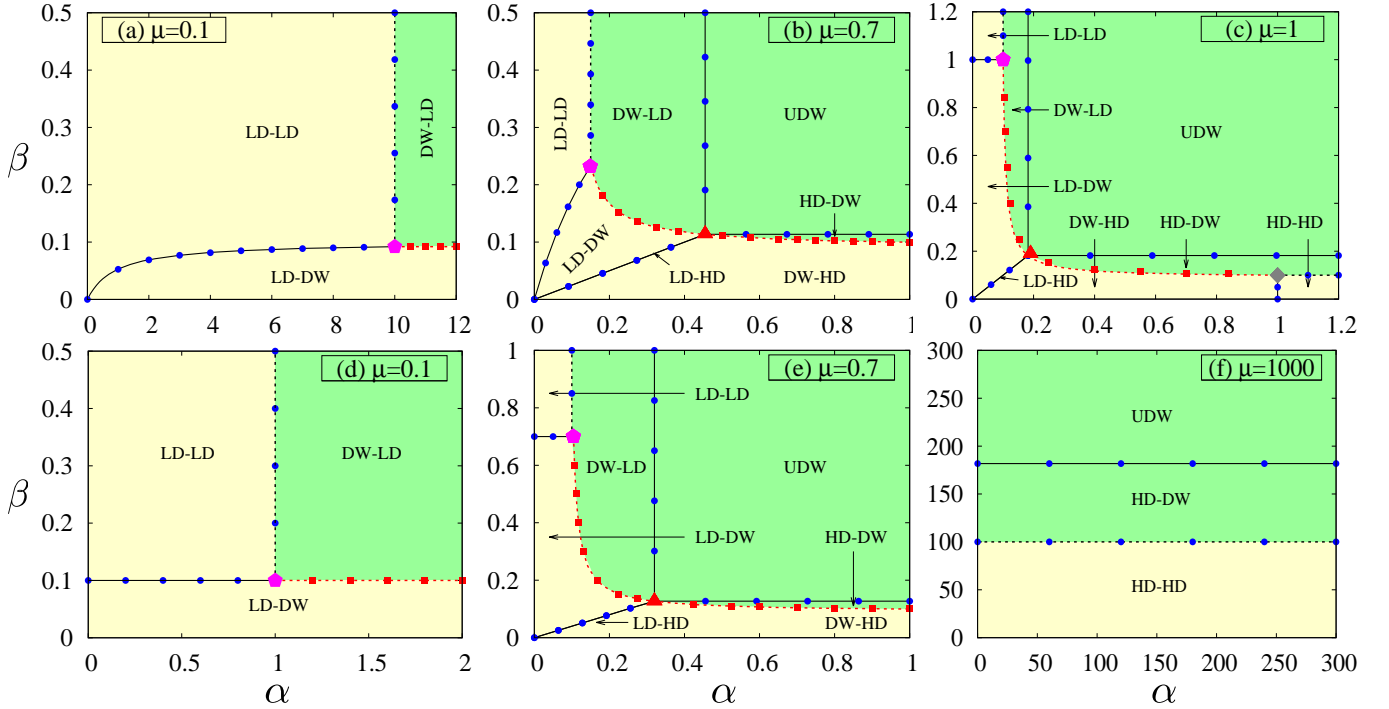


FIG. 2: Phase diagrams in the α - β plane for different μ at fixed $q = 0.1$ with reservoir-controlled regions (yellow) and defect-controlled regions (green). Upper Figs. 2(a-c) and lower Figs. 2(d-f) panels correspond to $N^* = L$ and $N^* = N_0$, respectively. LD-LD, HD-HD, LD-DW, DW-HD, DW-LD, HD-DW, UDW, and LD-HD (solid black line in Figs. 2(b), 2(c), and 2(e)) phases are obtained. Delocalized domain walls in both T_A and T_B form on the hyperbola (15) (red dashed line in Figs. 2(a-e)) between points (A) (magenta pentagon) and (B) (grey diamond) (see Table I in SM for their coordinates), with delocalization completely at $(\tilde{\alpha}, \tilde{\beta})$ (red triangle; see Eq. (17)) and partial elsewhere on (15). LDWs appear in the remaining DW phase regions. MFT (solid and dashed lines) and MCS (colored points) agree well.

phase. The boundary between DW-LD and UDW phases is thus found from $x_{w_1} = 0$ in Eq. (8) giving $\alpha(\mu - 1/2) = q/(1+q)$ for $N^* = L$, and $\alpha(1 - \mu/2) = q/(1+q)$ for $N^* = N_0$ (see Figs. 2(b), 2(c), and 2(e)).

With T_A , T_B fully in their HD and LD phases respectively (corresponding to a DW at $x = 1/2$), BLs of vanishing thickness form at $j = 1$ and $j = L$ (first and last sites of T_A and T_B), respectively. Assuming these are confined to a single site in the thermodynamic limit, current conservation gives the BL densities

$$\rho_1 = [1 + q/\{(1+q)\alpha(\mu - 1/2)\}]^{-1}, \quad (9)$$

$$\rho_L = [1 + \{(1+q)\beta(3/2 - \mu)\}/q]^{-1}. \quad (10)$$

As (α, β) grow, $\rho_1 \rightarrow 1, \rho_L \rightarrow 0$ eventually, without affecting the DW at $x = 1/2$ — giving the *universal DW* (UDW) phase. As $q \rightarrow 1$, the DW height ($\rho_{\text{HD}} - \rho_{\text{LD}} = (1-q)/(1+q)$, see Eq. (7)) gradually decreases vanishing at $q = 1$, yielding an MC phase with BLs at both ends. For larger μ , i.e., when there are more particles in the system, the LDW moves to T_B crossing the entry-end $x = 0$ of T_A (same as the exit-end $x = 1$ of T_B ; see Fig. 1), giving the HD-DW phase, and finally returns to $x = 1/2$ giving the HD-HD phase. Current conservation in UDW as well as in HD-DW phase gives

the associated densities $\rho_{\text{LD}} = q/(1+q) = 1 - \rho_{\text{HD}}$. PNC gives the LDW position in HD-DW phase:

$$x_{w_2} = \begin{cases} [5/2 - \mu(1+q) + q(1/2 - 1/\beta)]/(1-q), \\ (3/2 - \mu q/\beta - q/2)/(1-q), \end{cases} \quad (11)$$

for $N^* = L$ (top) and $N^* = N_0$ (bottom). Substituting $x_{w_2} = 1$ in Eq. (11) gives the boundary between UDW and HD-DW phases: $\beta(3/2 - \mu) = q/(1+q)$ for $N^* = L$, and $\beta = 2\mu q/(1+q)$ for $N^* = N_0$ (see Figs. 2(b), 2(c), 2(e), and 2(f)). Analogous to an open TASEP, densities in the HD-HD phase are $\rho_A = 1 - \beta_A$ and $\rho_B = 1 - \beta_{\text{eff}}(N_R) = \rho_A$, (current conservation). We get

$$\rho_{\text{HD-HD}} = \begin{cases} (1 - \beta + \mu\beta)/(1 + \beta), & N^* = L, \\ \mu/(\mu + \beta), & N^* = N_0. \end{cases} \quad (12)$$

independent of q . Furthermore, the boundary separating HD-HD phase from HD-DW phase is obtained by setting $x_{w_2} = 1/2$ in Eq. (11), thereby giving $(2 - \mu)\beta/(1 + \beta) = q/(1+q)$ for $N^* = L$, and $\mu q = \beta$ for $N^* = N_0$ (see Figs. 2(c) and 2(f)).

There is a second possibility for an LDW formation. Upon raising μ starting from the LD-LD phase, before hitting the threshold $\alpha_{\text{eff}} = q/(1+q)$, depending on the

parameters, α_{eff} can reach another threshold with $\alpha_{\text{eff}} = \beta_{\text{eff}}$, for which an LDW is formed at $x = 1$, giving the onset of the LD-DW phase. Further increase in μ pushes the LDW towards $x = 0$, going through the LD-DW, LD-HD (when the LDW is at $x = 1/2$) and DW-HD phases – finally reaching the HD-HD phase. With $\alpha_{\text{eff}} = \beta_{\text{eff}}$ in the DW phase, we get $f(N_R) = \beta/(\alpha + \beta)$, for both $N^* = L$ and N_0 , giving LDW densities as

$$\rho_{\text{LD}} = \alpha\beta/(\alpha + \beta) = 1 - \rho_{\text{HD}}, \quad (13)$$

independent of q . By PNC, the LDW location x_{w_3} is

$$x_{w_3} = \begin{cases} [\alpha + 2\beta - \mu(\alpha + \beta) - \alpha\beta]/(\alpha + \beta - 2\alpha\beta), \\ (\alpha + \beta - \mu\alpha - \alpha\beta)/(\alpha + \beta - 2\alpha\beta), \end{cases} \quad (14)$$

for $N^* = L$ (top) and $N^* = N_0$ (bottom). The LDW shape being controlled by $\alpha, \beta, \mu, f(N_R)$ is clearly *nonuniversal*. Substituting $x_{w_3} = 1$ in Eq. (14) provides the boundary between LD-LD and LD-DW phases: $\mu/(1 + \alpha) = \beta/(\alpha + \beta)$ for $N^* = L$ and $\beta = \mu$ for $N^* = N_0$ (see Figs. 2(a)-2(e)). Next, $x_{w_3} = 1/2$ in Eq. (14) gives the boundary between LD-DW and LD-HD phases: $\beta/(\alpha + \beta) = \mu - 1/2$ for $N^* = L$ and $\beta/(\alpha + \beta) = 1 - 1/2\mu$ for $N^* = N_0$, which are also boundaries between LD-HD and DW-HD phases (see Figs. 2(b), 2(c), and 2(e)). Lastly, the boundary between DW-HD and HD-HD phases is obtained by substituting $x_{w_3} = 0$ in Eq. (14): $\alpha/(\alpha + \beta) = (2 - \mu)/(1 + \beta)$ for $N^* = L$ and $\alpha/(\alpha + \beta) = 1/(\mu + \beta)$ for $N^* = N_0$.

A minimum current principle [32] determines whether DWs are defect- or reservoir-induced: when the corresponding stationary currents $J_{\text{def}} = q/(1 + q)^2 < (>) J_{\text{res}} = \alpha\beta/(\alpha + \beta)[1 - \alpha\beta/(\alpha + \beta)]$, DWs are controlled by the defect (reservoir). This gives the surface

$$\alpha\beta/(\alpha + \beta) = q/(1 + q) \quad (15)$$

that separates the two regimes. Hyperbola (15) along which DDWs appear has one or two endpoints in the $\alpha\beta$ plane depending on μ and q (see SM for details). This curve demarcates the boundary between the LD-DW and DW-LD as well as DW-HD and HD-DW phases. Accordingly, DW-LD and HD-DW phases appear in the defect-controlled (green) region, while LD-DW and DW-HD appear in the reservoir-controlled (yellow) region in Fig. 2; see also the movies in SM [47].

The LD-DW and DW-HD phases meet along the LD-HD phase line $F(\alpha, \beta, \mu) = 0$, obtained by setting $x_{w_3} = 1/2$ in Eq. (14), giving

$$F(\alpha, \beta, \mu) = \begin{cases} [(\alpha + 3\beta)/2(\alpha + \beta)] - \mu, & N^* = L, \\ [(\alpha + \beta)/2\alpha] - \mu, & N^* = N_0, \end{cases} \quad (16)$$

terminating at

$$(\tilde{\alpha}, \tilde{\beta}) = \begin{cases} 2q/(1 + q)(1/(2\mu - 1), 1/(3 - 2\mu)), & N^* = L \\ 2\mu q/(1 + q)(1/(2\mu - 1), 1), & N^* = N_0 \end{cases} \quad (17)$$

where $(\tilde{\alpha}, \tilde{\beta})$ is the intersection of $F = 0$ and (15).

Intriguingly, when $J_{\text{def}} = J_{\text{res}}$, i.e., the defect “competes” with the reservoir, a new kind of state, *a pair of DDWs*, emerges for μ satisfying the conditions for DW formation due to both the defect and reservoir. Following the logic of the LDW formation due to the defect or reservoir, we expect one DW, say at $x = x_w^{\text{def}}$ in T_A due to and behind the defect and another DW at $x = x_w^{\text{res}}$ in T_B due to and behind the reservoir. A complete description of the state of the system then requires enumeration of both x_w^{def} and x_w^{res} . However, with just PNC condition, only a linear relation between x_w^{def} and x_w^{res} is obtained, implying that any pair of $(x_w^{\text{def}}, x_w^{\text{res}})$ satisfying PNC is a valid solution. Further, the inherent stochasticity of the underlying microscopic dynamics ensures that all such pairs of $(x_w^{\text{def}}, x_w^{\text{res}})$ are visited over time. As a result, we get one DDW in each of T_A and T_B [19]. See Fig. 3 and phase diagrams in Figs. 2(a)-2(e) (red dashed). At $(\tilde{\alpha}, \tilde{\beta})$, DDWs are fully delocalized across T_A and T_B (red triangular point in Figs. 2(b), 2(c), 2(e)). Moving away from $(\tilde{\alpha}, \tilde{\beta})$ on (15), their spans gradually decrease, vanishing at the endpoints of (15). Geometric constructions of the DDW profiles [47] that depend on the parameters and f (hence nonuniversal) show good agreement with the MCS results; see Fig. 4. Phase transitions across (15) are characterized by a jump in ρ , indicating a discontinuous transition; ρ varies continuously across other phase boundaries.

We have thus shown that a TASEP with finite resources and a bottleneck admits a universal DW for sufficiently large α, β and μ . A DW for other choices of the model parameters can also exist, but is not universal. These results are robust and hold true for a reservoir with finite or infinite carrying capacity. Experimental measurements of a UDW should fail to resolve the corresponding model parameters and the specific choice of $f(N_R)$, reminiscent of universal critical phenomena [46]. The model also admits a pair of DDWs, whose degree of delocalization can be varied smoothly by tuning the model parameters, and are nonuniversal. It will be interesting to study the degree of universality of the fluctuations in the UDW phase by systematically going beyond MFT [50, 51].

Acknowledgement:- A.B. thanks Alexander von Humboldt Stiftung (Germany) for partial financial support through their research group linkage programme (2024).

* Electronic address: isourav81@gmail.com

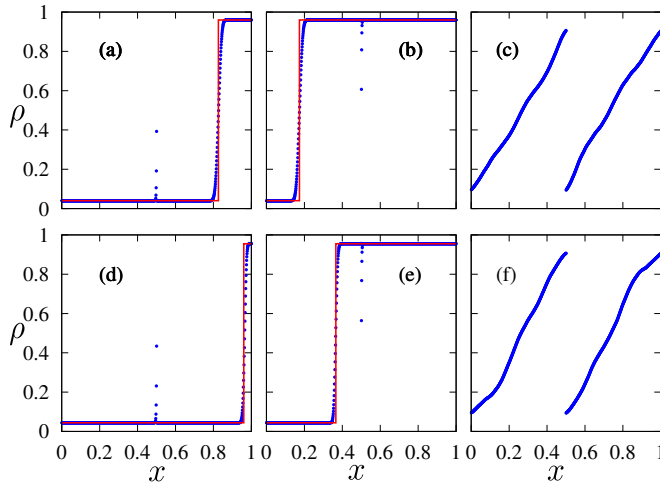


FIG. 3: LDWs (subplots (a), (b), (d), and (e)) and DDWs (subplots (c), (f)) are shown for $q = 0.1$. System size $L = 1000$ and 10^7 Monte Carlo steps are taken for time-average. MFT (red solid lines) and MCS (blue circular points) results match well. Subplots (a), (b), and (c) correspond to $N^* = L$, while (d), (e), and (f) correspond to $N^* = N_0$. (a) $\alpha = 0.05$, $\beta = 0.2$, $\mu = 1$; (b) $\alpha = 0.2$, $\beta = 0.05$, $\mu = 1$; (c) $\alpha = \beta = 0.19$, $\mu = 1$; (d) $\alpha = 0.05$, $\beta = 0.4$, $\mu = 0.7$; (e) $\alpha = 0.4$, $\beta = 0.05$, $\mu = 0.7$; and (f) $\alpha = 0.333$, $\beta = 0.1332$, $\mu = 0.7$.

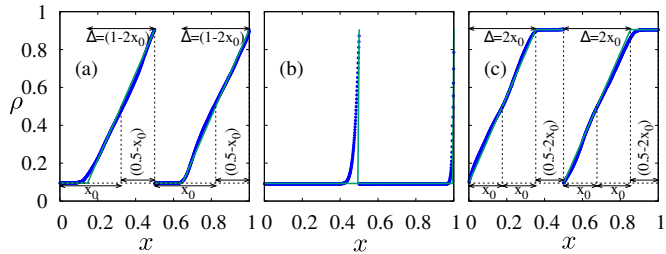


FIG. 4: Partially delocalized DDWs for parameters on (15) away from $(\tilde{\alpha}, \tilde{\beta})$ for $N^* = L$. (a) $\alpha = 0.154, \beta = 0.25$; (b) $\alpha = 0.103, \beta = 0.95$; and (c) $\alpha = 0.25, \beta = 0.154$ with fixed $\mu = 1, q = 0.1$ for all. MCS results (blue circles) match very well with geometrical constructions (green solid lines) of the DDW profiles, see Eqs. (20) and (22) in SM for the position and span of DDWs.

[†] Electronic address: abhik.123@gmail.com, abhik.basu@saha.ac.in

- [1] D. Chowdhury, L. Santen and A. Schadschneider, Phys. Rep. 329, 199 (2000).
- [2] D. Helbing, Rev. Mod. Phys. **73**, 1067 (2001).
- [3] S. E. Wells, E. Hillner, R. D. Vale and A. B. Sachs, Mol. Cell. 2, 135 (1998).
- [4] S. Wang, K. S. Browning and W. A. Miller, EMBO J. 16, 4107 (1997).
- [5] Y. Nakamura, T. Gojobori, and T. Ikemura, Nucleic Acids Res. 28 292 (2000).
- [6] T. Karzig and F. von Oppen, Phys. Rev. B 81, 045317 (2010).
- [7] J. Krug, “Boundary-induced phase transitions in driven diffusive systems”, Phys. Rev. Lett. 67, 1882 (1991).
- [8] B. Derrida, S. A. Janowsky, J. L. Lebowitz, and E. R.

- Speer, “Exact solution of the totally asymmetric simple exclusion process: Shock profiles”, J Stat Phys , 813–842.
- [9] B. Derrida and M. R. Evans, “Exact correlation functions in an asymmetric exclusion model with open boundaries”, Journal de Physique I 3, 311–322 (1993).
- [10] C. T. MacDonald, J. H. Gibbs, and A. C. Pipkin, Kinetics of biopolymerization on nucleic acid templates, Biopolymers **6**, 1 (1968).
- [11] B. Derrida, M. R. Evans, V. Hakim, and V. Pasquier, Exact solution of a 1d asymmetric exclusion model using a matrix formulation, J. Phys. A: Math. and Gen. 26, 1493–1517 (1993).
- [12] R. A. Blythe and M. R. Evans, Nonequilibrium steady states of matrix-product form: a solver’s guide, J. Phys. A 40, R333 (2007).
- [13] T Chou, K Mallick, and R K P Zia, Non-equilibrium statistical mechanics: from a paradigmatic model to biological transport, Rep. Prog. Phys. **74**, 116601 (2011).
- [14] S. A. Janowsky and J. L. Lebowitz, Finite-size effects and shock fluctuations in the asymmetric simple- exclusion process, Phys. Rev. A 45, 618 (1992).
- [15] G. Tripathy and M. Barma, Driven lattice gases with quenched disorder: Exact results and different macroscopic regimes, Phys. Rev. E **58**, 1911 (1998).
- [16] P. Pierobon, M. Mobilia, R. Kouyos, and E. Frey, Bottleneck-induced transitions in a minimal model for intracellular transport, Phys. Rev. E **74**, 031906 (2006).
- [17] H. Hinsch and E. Frey, “Bulk-driven nonequilibrium phase transitions in a mesoscopic ring”, Phys. Rev. Lett. 97, 095701 (2006).
- [18] R. Chatterjee, A. K. Chandra, and A. Basu, Phase transition and phase coexistence in coupled rings with driven exclusion processes, Phys. Rev. E 87, 032157 (2013).
- [19] N. Sarkar and A. Basu, Nonequilibrium steady states in asymmetric exclusion processes on a ring with bottlenecks, Phys. Rev. E **90**, 022109 (2014).
- [20] T. Banerjee, N. Sarkar and A. Basu, Generic nonequilibrium steady states in an exclusion process on an inhomogeneous ring, J. Stat. Mech. J. Stat. Mech. P01024 (2015).
- [21] R. Chatterjee, A. K. Chandra, and A. Basu, Asymmetric exclusion processes on a closed network with bottlenecks, J. Stat. Mech. (2015) P01012.
- [22] T. Banerjee and A. Basu, Smooth or shock: Universality in closed inhomogeneous driven single file motions, Phys. Rev. Research **2**, 013025 (2020).
- [23] P. Roy, A.K. Chandra, and A. Basu, Pinned or moving: states of a single shock in a ring, Phys. Rev. E **102**, 012105 (2020).
- [24] A. Goswami, R. Chatterjee, and S. Mukherjee, Defect versus defect: stationary states of single file marching in periodic landscapes with road blocks, arXiv: 2402.08499.
- [25] B. Alberts, A. Johnson, P. Walter, and J. Lewis, Molecular Biology of the Cell, 5th ed. (Garland Publishing Inc., New York, 2008).
- [26] D. A. Adams, B. Schmittmann, and R. K. P. Zia, Far from equilibrium transport with constrained resources, J. Stat. Mech. (2008) P06009.
- [27] L. Jonathan Cook and R. K. P. Zia, Feedback and fluctuations in a totally asymmetric simple exclusion process with finite resources, J. Stat. Mech. (2009) P02012.
- [28] L. J. Cook, R. K. P. Zia, and B. Schmittmann, Competition between multiple totally asymmetric simple exclusion processes for a finite pool of resources, Phys. Rev. E

80, 031142 (2009).

[29] A. Haldar, P. Roy, and A. Basu, Asymmetric exclusion processes with fixed resources: Reservoir crowding and steady states, *Phys. Rev. E* **104**, 034106 (2021).

[30] S. Pal, P. Roy, and A. Basu, Availability, storage capacity, and diffusion: Stationary states of an asymmetric exclusion process connected to two reservoirs, *Phys. Rev. E* **110**, 054104 (2024).

[31] S. Pal, P. Roy, and A. Basu, Distributed fixed resources exchanging particles: Phases of an asymmetric exclusion process connected to two reservoirs, *Phys. Rev. E* **111**, 034109 (2025).

[32] A. Haldar, P. Roy, E. Frey, and A. Basu, Availability versus carrying capacity: Phases of asymmetric exclusion processes competing for finite pools of resources, *Phys. Rev. E* **111**, 014154 (2025).

[33] R. Brockmann, A. Beyer, J. J. Heinisch, and T. Wilhelm, Posttranscriptional Expression Regulation: What Determines Translation Rates?, *PLOS Comput. Biol.* **3**, e57 (2007).

[34] I. J. Purvis, A. J. E. Bettany, T. C. Santiago, J. R. Coggins, K. Duncan, R. Eason, and A. J. P. Brown, The efficiency of folding of some proteins is increased by controlled rates of translation in vivo: A hypothesis, *J. Mol. Biol.* **193**, 413 (1987).

[35] M. C. Romano, M. Thiel, I. Stansfield, and C. Grebogi, Queueing Phase Transition: Theory of Translation, *Phys. Rev. Lett.* **102**, 198104 (2009).

[36] M. A. Sorensen, C. G. Kurland and S. Pedersen, Codon usage determines translation rate in *Escherichia coli*, *J. Mol. Biol.* **207**, 365 (1989).

[37] T. Chou, Ribosome Recycling, Diffusion, and mRNA Loop Formation in Translational Regulation, *Biophys. J.* **85**, 755 (2003).

[38] S. E. Wells, E. Hillner, R. D. Vale and A. B. Sachs, Circularization of mRNA by Eukaryotic Translation Initiation Factors, *Mol. Cell* **2**, 135 (1998).

[39] G. S. Kopeina et al, Step-wise formation of eukaryotic double-row polyribosomes and circular translation of polysomal mRNA, *Nucleic Acids Res.* **36**, 2476 (2008).

[40] Robinson M et al, Codon usage can affect efficiency of translation of genes in *Escherichia coli*, *Nucleic Acids Res.* **12**, 6663 (1984).

[41] D. A. Phoenix and E. Korotkov, Evidence of rare codon clusters within *Escherichia coli* coding regions, *FEMS Microbiol. Lett.* **155**, 63 (1997).

[42] D. Chowdhury, L. Santen and A. Schadschneider, Statistical physics of vehicular traffic and some related systems, *Phys. Rep.* **329**, 199 (2000).

[43] D. Helbing, Traffic and related self-driven many-particle systems, *Rev. Mod. Phys.* **73**, 1067 (2001).

[44] Steady state properties are not affected with the precise location of the point defect, which is, however, placed in the bulk far from the boundaries to avoid any boundary effect.

[45] C. A. Brackley, M.C. Romano and M. Thiel, The Dynamics of Supply and Demand in mRNA Translation, *PLoS Computational Biology* **7**, e1002203 (2011).

[46] P. M. Chaikin and T. C. Lubensky, Principles of Condensed Matter Physics (Cambridge University Press, Cambridge, 2000).

[47] Supplemental Material.

[48] C. A. Brackley, M. C. Romano, and M. Thiel, Slow sites in an exclusion process with limited resources, *Phys. Rev. E* **82**, 051920 (2010).

[49] L. J. Cook, J. J. Dong, and A. LaFleur, Interplay between finite resources and a local defect in an asymmetric simple exclusion process, *Phys. Rev. E* **88**, 042127 (2013).

[50] L. Bertini, A. D. Sole, D. Gabrielli, G. Jona-Lasinio and C. Landim, Macroscopic fluctuation theory, *Rev. Mod. Phys.* **87**, 593 (2015).

[51] B. Doyon, G. Perfetto, T. Sasamoto, and T. Yoshimura, Ballistic macroscopic fluctuation theory, *SciPost Phys.* **15**, 136 (2023).

DELOCALIZATION OF THE DOMAIN WALLS

This section investigates the delocalization of domain walls along the hyperbola (15), which separates defect-controlled (green) and reservoir-controlled regions (yellow) (see Fig. 2). Along this hyperbola, DDWs can emerge within a region of the α - β plane, the extent of which depends explicitly on the value of μ and q . Complete delocalization occurs at the point $(\tilde{\alpha}, \tilde{\beta})$ given by Eq. (17), where all phases meet (red triangle in Figs. 2(b), 2(c), and 2(e)). Moving away from this point on both sides, span of DDWs gradually decreases and eventually vanishes at the boundaries essentially taking the form of boundary layers. Full delocalization is seen in Fig. 3(c) ($\alpha = \beta = 0.19$, $\mu = 1$, $q = 0.1$, $N^* = L$) and Fig. 3(f) ($\alpha = 0.333$, $\beta = 0.1332$, $\mu = 0.7$, $q = 0.1$, $N^* = N_0$). Partial delocalization for $N^* = L$ is shown in Fig. 4(a) ($\alpha = 0.154$, $\beta = 0.25$, $\mu = 1$, $q = 0.1$), Fig. 4(b) ($\alpha = 0.103$, $\beta = 0.95$, $\mu = 1$, $q = 0.1$) on one side of the point $(\tilde{\alpha}, \tilde{\beta})$, and in Fig. 4(c) ($\alpha = 0.25$, $\beta = 0.154$, $\mu = 1$, $q = 0.1$) on the other side. Clearly, as we move away from $(\tilde{\alpha}, \tilde{\beta})$, the degree of delocalization decreases, see Figs. 4(a) and 4(b). The cases in Figs. 4(a) and (c) are related by particle-hole symmetry.

The endpoints of the hyperbola (15) in the α - β plane, within which DDWs are observed, are denoted as points (A) and (B) (see Fig. 2), coordinates of which can be determined as follows. Point (A) lies at the junction of the LD-LD/LD-DW, LD-LD/DW-LD, and LD-DW/DW-LD phase boundaries, whereas point (B) is located at the intersection of the HD-HD/DW-HD, HD-HD/HD-DW, and DW-HD/HD-DW boundaries. These boundaries are precisely obtained for both cases $N^* = L$ and $N^* = N_0$, as detailed in the main paper. The coordinates of points (A) and (B) for each case, as determined above, are listed below in Table I:

Hence, the coordinates of points (A) and (B) depend ex-

plicitly on the parameters μ and q . Since $\alpha, \beta > 0$ by

TABLE I: Coordinates of points (A) and (B) for two representative cases

Point Case \	(A)	(B)
$N^* = L$	$\left(\alpha = \frac{q}{\mu(1+q)-q}, \beta = \frac{q}{1+2q-\mu(1+q)} \right)$	$\left(\alpha = \frac{q}{\mu(1+q)-1}, \beta = \frac{q}{2+q-\mu(1+q)} \right)$
$N^* = N_0$	$\left(\alpha = \frac{\mu q}{\mu(1+q)-q}, \beta = \mu \right)$	$\left(\alpha = \frac{\mu q}{\mu(1+q)-1}, \beta = \mu q \right)$

definition, this imposes the following conditions in Table II for the existence of points (A) and (B) in the two

cases:

TABLE II: Conditions for the existence of points (A) and (B) for two representative cases

Point Case \	(A)	(B)
$N^* = L$	$\frac{q}{1+q} < \mu < \frac{1+2q}{1+q}$	$\frac{1}{1+q} < \mu < \frac{2+q}{1+q}$
$N^* = N_0$	$\mu > \frac{q}{1+q}$	$\mu > \frac{1}{1+q}$

For example, for $N^* = L$ in Fig. 2(a) and Fig. 2(b), where $\mu = q = 0.1$ and $\mu = 0.7$, $q = 0.1$ respectively, only point (A) is observed, while point (B) is absent. In contrast, in Fig. 2(c) with $\mu = 1$, $q = 0.1$, both points (A) and (B) are present. For $N^* = N_0$, in Fig. 2(d) and Fig. 2(e), where $\mu = q = 0.1$ and $\mu = 0.7$, $q = 0.1$ respectively, point (A) is observed, while point (B) is not visible. In Fig. 2(f), both points (A) and (B) are present but appear at very small values of α , which are not shown in the phase diagram. These observations are in agreement with the conditions obtained in Table II.

We now analyze the position and spatial span of DDWs occurring on (15) to determine their degree of delocalization. Consider a pair of DDWs located at positions x_0 in T_A and $1/2+x_0$ in T_B . Current conservation ($J_{\text{def}} = J_{\text{res}}$) on (15) yields

$$\rho_{\text{LD}} = \frac{\alpha\beta}{\alpha+\beta} = \frac{q}{1+q} = 1 - \rho_{\text{HD}}, \quad (18)$$

for both $N^* = L$ and $N^* = N_0$, see Eqs. (7) and (13). We apply PNC separately for $N^* = L$ and $N^* = N_0$ to obtain the average position of the DDW. Recall that the filling factor is defined as $\mu = N_0/L$, and the low-density in both defect- and reservoir-controlled DW phases reads $\rho_{\text{LD}} = \alpha N_R/L$ for $N^* = L$, and $\rho_{\text{LD}} = \alpha N_R/N_0$ for $N^* = N_0$. Denoting the particle numbers in T_A and T_B

as N_A and N_B , respectively, PNC reads for $N^* = L$:

$$\begin{aligned} N_0 &= N_R + N_A + N_B, \\ \implies \mu &= \frac{\rho_{\text{LD}}}{\alpha} + \int_0^{x_0} \rho_{\text{LD}} dx + \int_{x_0}^{1/2} \rho_{\text{HD}} dx \\ &\quad + \int_{1/2}^{1/2+x_0} \rho_{\text{LD}} dx + \int_{1/2+x_0}^1 \rho_{\text{HD}} dx. \end{aligned} \quad (19)$$

Solving Eq. (19) for x_0 , we obtain

$$x_0 = \frac{1 - \mu - \rho_{\text{LD}} (1 - \frac{1}{\alpha})}{2(1 - 2\rho_{\text{LD}})}, \quad (20)$$

where ρ_{LD} is given by Eq. (18). Similarly, for $N^* = N_0$, we get

$$x_0 = \frac{1 - \mu - \rho_{\text{LD}} (1 - \frac{\mu}{\alpha})}{2(1 - 2\rho_{\text{LD}})}, \quad (21)$$

with ρ_{LD} again given by Eq. (18). Depending on α, β for fixed values of μ and q , the DW position, x_0 , obtained in Eqs. (20) and (21) can be greater than (Figs. 4(a) and 4(b)), equal to (Figs. 3(c) and 3(f)), or less than (Fig. 4(c)) 1/4. DDW span, Δ , is obtained from the geometric constructions of DDWs in Fig. 4 as

$$\Delta = \begin{cases} 1 - 2x_0, & \text{for } x_0 > 1/4, \\ 1/2, & \text{for } x_0 = 1/4, \\ 2x_0, & \text{for } x_0 < 1/4, \end{cases} \quad (22)$$

for both $N^* = L$ and $N^* = N_0$.

We will now compare x_0 and Δ obtained from MCS in Fig. 4 with those obtained analytically in Eqs. (20), (21), and (22). We consider only the case $N^* = L$ with $\mu = 1, q = 0.1$ for which the point of complete delocalization is $(\tilde{\alpha}, \tilde{\beta}) = (0.19, 0.19)$, see Eq. (17). In Fig. 4(a) with $\alpha = 0.154, \beta = 0.25$, we get $x_0 = 0.32$ and $\Delta = 1 - 2x_0 = 0.36$. In Fig. 4(b), with $\alpha = 0.103, \beta = 0.95$, we find $x_0 = 0.49$

and $\Delta = 1 - 2x_0 = 0.02$. These results indicate that the degree of delocalization of the DW decreases as one moves away from the point of complete delocalization, i.e., $(\tilde{\alpha}, \tilde{\beta})$. Finally, in Fig. 4(c), for $\alpha = 0.25, \beta = 0.154$, we obtain $x_0 = 0.18$ and $\Delta = 2x_0 = 0.36$. All these analytical results match very well with the values of x_0 and Δ obtained by MCS.